



Kinetics of spinodal decomposition in driven nanocrystalline alloys

I.K. Razumov*, Yu. N. Gornostyrev, A. Ye. Yermakov

Institute of Metal Physics, Ural Branch of RAS, 18 Kovalevskaya Street, Ekaterinburg 620041, Russia

Abstract

The effect of grain boundaries (GB) on decomposition of solid solution was investigated in the framework generalized lattice gas model taking into account both local variation of chemical potential and the increase of diffusion mobility near GB. It was shown that nonequilibrium GB can essentially change the phase equilibrium of alloy and surface directed spinodal decomposition (SDSD) caused by GB determines the precipitation morphology in nanograined materials. The increase of atomic mobility near GB can result in formation of lamellar structure propagating from GB to inside the grains and variation in morphology from lamellar to drop-like type structure with composition.

© 2006 Published by Elsevier B.V.

Keywords: Grain boundaries; Diffusion; Composition fluctuations; Phase transitions

1. Introduction

It is well-known that grain boundaries (GB) play an important role in phase equilibrium of alloys. GB's are considered as preferable places for segregation of one of the components and stimulate heterogeneous nucleation of a new phase [1]. Recently attention was drawn to another aspect of this problem, i.e. the role of inner interfaces/or boundaries in transformation kinetics and microstructure formation [2]. It was found that the interfaces can stimulate the appearance of concentration waves propagating inside a sample when homogeneous alloy state is unstable with respect to spinodal decomposition. This phenomenon has been thoroughly studied lately (see review [3]) and was called surface directed spinodal decomposition (SDSD). In the case of SDSD a new phase is formed with alternating domains in repeating geometry [4]. As was shown in [5], in some cases the concentration inhomogeneities can reach macroscopic level.

It follows that the role of GB's in alloys phase instability will grow drastically when grain size decreases to nanoscale and fraction of atoms in GB region become comparable with that of the core. In particular, the observation of unusual phase transformations in nanograined materials at intensive plastic deformation

[6] confirms this point of view. Though the question of physical mechanisms of the phase instability under intensive plastic deformation is still under discussions, there is no doubt that kinetics and thermodynamic factors [7] should be taken into account for explanation of decomposition phenomena in systems of freely miscible components or formation of new nonequilibrium phases [8].

As it was stressed in [7], the decrease of grain size to nanometer range may stimulate the decomposition even in a stable solid solution. An essential condition for realization of size effect is a long-range chemical potential perturbation produced by GB. This approach [7] is distinguished from conventional SDSD models [3] where a change of chemical potential is strictly localized on GB. The important role of the surface in redistribution of atoms is shown in [5] where the long-range effect was ascribed to elastic strains. We can also expect the long-range influence of GB on spinodal decomposition since the GB in nanograin materials after severe plastic deformation are highly nonequilibrium and can create significant lattice distortion [9].

In this paper we develop the model [7,8] taking into account the microscopic mechanism of interaction between GB and solute atoms. We generalize a lattice gas model for the inhomogeneous case where parameters of chemical bond are changed near GB. This allows us to consider in a unified scheme GB segregations of one component and the change in diffusion mobility in region adjacent to the boundary. The developed model reproduces main features of SDSD in detail and also predicts the new

* Corresponding author. Tel.: +7 343 378 3669; fax: +7 343 374 5244.
E-mail address: rik@imp.uran.ru (I.K. Razumov).

phenomena such as, for instance, dissolution of precipitates in small grains.

2. Model description

For description of decomposition kinetics we use ABv model of the lattice gas (see [10] and reviews [11,12] in which A, B correspond to alloy components and v is a vacancy. Kinetic equation for concentrations $C_i^\alpha = \langle n_i^\alpha \rangle$ (n_i^α is occupation numbers, 1 in case if atom $\alpha = A, B$ placed in i position and 0 in opposite case)) is deduced from the master kinetic equation for ABv model in mean field approximation [5,10–12]. As a result we get a discrete analog of Fick's equation:

$$\frac{\partial C_i^\alpha(t)}{\partial t} = - \sum_j J_{ij}^\alpha(t), \quad J_{ij}^\alpha = -\omega_{ji}^\alpha C_j^\alpha C_i^v + \omega_{ij}^\alpha C_i^\alpha C_j^v \quad (1)$$

describing the evolution of the concentrations C_i^α in time, where

$$\omega_{ij}^\alpha = \omega_0^\alpha \exp\left(\frac{E_{i\alpha}^{\text{int}}}{kT}\right), \quad \omega_0^\alpha = v_0^\alpha \exp\left(\frac{-U_\alpha}{kT}\right) \quad (2)$$

are frequencies of atom jumps into a neighboring vacancy site ($i \rightarrow j$); U_α is atomic energy in a “saddle” point and it does not depend on configuration:

$$E_{i\alpha}^{\text{int}} = \sum_k [\varphi^{\alpha A}(r_{ik}) C_{i+k}^A + \varphi^{\alpha B}(r_{ik}) C_{i+k}^B] \quad (3)$$

is interaction energy of atom i (in initial site before jump); $\varphi^{\alpha\beta}(r)$ is pair interaction energy of α, β atoms at a distance r .

Assuming that concentrations $C^\alpha(\mathbf{r})$ vary slowly on the scale of lattice parameter a , i.e. $C^\alpha(\mathbf{r} + \mathbf{a}) \approx C^\alpha(\mathbf{r}) + \mathbf{a} \cdot \nabla C^\alpha(\mathbf{r})$, Eq. (1) can be presented in the form:

$$\frac{\partial C^\alpha(\mathbf{r}, t)}{\partial t} = -\nabla \cdot \mathbf{J}^\alpha(\mathbf{r}, t) \quad (4)$$

where the flux is determined by the following:

$$\mathbf{J}^\alpha = \omega^\alpha C^\alpha \nabla C^v - \omega^\alpha C^v \nabla C^\alpha - C^\alpha C^v \nabla \omega^\alpha \quad (5)$$

where C^α and C^v are concentrations of alloy components and vacancies and obey the relations $C^A + C^B + C^v = 1$ and $\mathbf{J}^A + \mathbf{J}^B + \mathbf{J}^v = 0$. In this approximation the interaction energy (3) is determined by expression:

$$E_\alpha^{\text{int}}(\mathbf{r}) = (\Phi_{\alpha B} - \Phi_{\alpha A})(C^\beta(\mathbf{r}) + R_\alpha^2 \Delta C^\beta(\mathbf{r})) + \Phi_{\alpha\alpha} \quad (6)$$

where

$$\Phi_{\alpha\beta} = \sum_k \varphi^{\alpha\beta}(|\mathbf{r} - \mathbf{r}_k|), \quad R_\alpha^2 = \frac{1}{2(\Phi_{\alpha B} - \Phi_{\alpha A})} \\ \times \sum_k r_k^2 (\varphi^{\alpha B}(|\mathbf{r} - \mathbf{r}_k|) - \varphi^{\alpha A}(|\mathbf{r} - \mathbf{r}_k|))$$

In an ideal homogeneous lattice these values $\Phi_{\alpha\beta}, R_\alpha$ are identical in any position ($\Phi_{\alpha\beta} = \text{const}, R_\alpha = \text{const}$). But deformation near defects or nonequilibrium grain boundaries destroy the equivalence of lattice sites. Therefore, we assume that

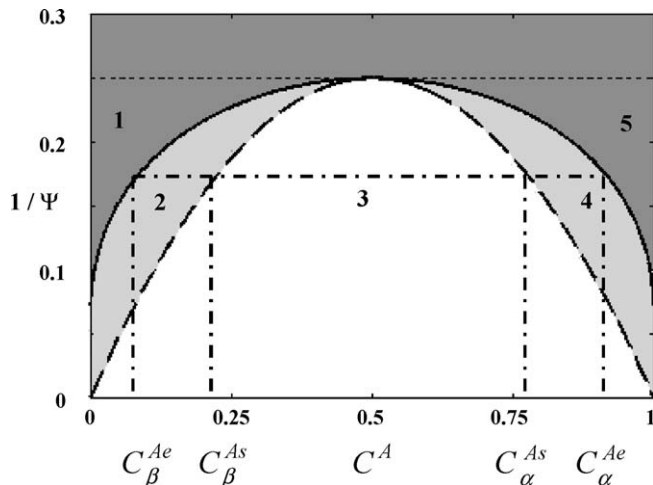


Fig. 1. Equilibrium phase diagram of a regular solid solution. Solid line corresponds to a solubility curve, dotted line to spinodal.

$\Phi_{\alpha\beta} = \Phi_{\alpha\beta}(\mathbf{r})$ and $\Phi_{\alpha\beta}(\mathbf{r}) = \Phi_{\alpha\beta}^{(0)} + \delta\Phi_{\alpha\beta}(\mathbf{r})$, where $\Phi_{\alpha\beta}^{(0)}$ corresponds to the ideal lattice and dependence $\delta\Phi_{\alpha\beta}(\mathbf{r})$ is determined by a lattice deformations.

In the present paper we suppose that fluxes of nonequilibrium vacancies are absent and we accept that $\mathbf{J}^v \rightarrow 0$; $\mathbf{J}^A = -\mathbf{J}^B$. Plugging Eqs. (6) and (2) in (5) we get:

$$\mathbf{J}^\alpha = -\frac{\omega^\alpha \omega^\beta C^v}{(\omega^\alpha C^\alpha + \omega^\beta C^\beta)} \left[(1 - \Psi C^\alpha C^\beta) \nabla C^\alpha + \frac{1}{2} C^\alpha C^\beta (\nabla \phi^\alpha + (1 - 2C^\alpha) \nabla \Psi - R^2 \nabla (\Psi \Delta C^\alpha)) \right] \quad (7)$$

where $\Psi = (2\Phi_{AB} - \Phi_{AA} - \Phi_{BB})/kT$ is dimensionless energy of mixing and $\nabla \phi^\alpha = (\Phi_{\alpha\alpha} - \Phi_{\beta\beta})/kT$ is the so-called asymmetric potential [12].

Substituting (7) in (4) we obtain a kinetic equation of generalized Cahn–Hilliard model [13] for heterogeneous systems in which thermodynamic parameters Ψ and ϕ^α vary in space.

The term proportional to ΔC^α in (7) has the same sense as a contribution of boundaries to concentration heterogeneities in Cahn–Hilliard equation [13]. The first item describes normal diffusion processes, when $1 - \Psi C_A C_B > 0$ and it leads to decomposition if alloy parameters cross the spinodal (in this case $1 - \Psi C_A C_B$ changes sign). The other terms describe the additive stimulus of decomposition due to the system heterogeneity and hence, it gives microscopic expression for the chemical potential variation. Besides, $\omega^\alpha = \omega^\alpha(\mathbf{r})$ determined by expressions (2), (6) describes the atomic mobility near GB. We assume that vacancy concentration C^v is a constant while time scale of decomposition kinetics is determined by the choice of the C^v value.

In an infinite ideal lattice at $\Psi < 0$ concentrations distribution is homogeneous for the single equilibrium state. At $\Psi < 0$ an alloy has an intrinsic thermodynamic stimulus for decomposition and transformation kinetics are determined by the position of alloy parameters on a phase diagram (Fig. 1). A regular solid solution solubility and spinodal curves are described by equations: $\ln(C^A/C^B) = \Psi(2C^A - 1)/2$ and $1 - \Psi C^A(1 - C^A) = 0$, respectively. The study of decomposition kinetics in presence

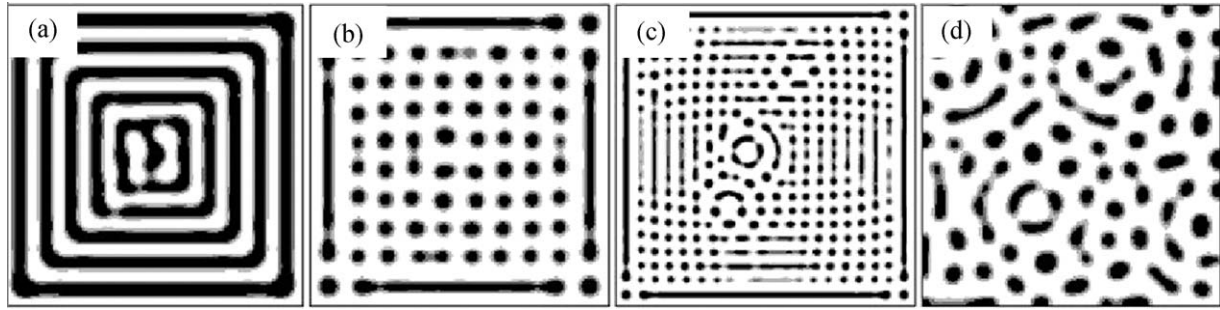


Fig. 2. Wave decomposition stage stimulated by segregations on GB (a–c) at $\delta\phi = 0.25\phi_0$ and for no perturbation on GB (d). Fragments (a), (b–d) show “stripe-like” and “drop-like” decomposition mechanisms at $C^{A0} = 0.5$ and $C^{A0} = 0.3$, respectively. $\Psi_0 = 8$, $\phi_0 = -2$, $\xi = R$, $\tau = 5$ $L = 100R$ (a, b and d), $L = 200R$ (c).

of GB was carried out by numerical integration of Eqs. (4) and (7) for square grain ($L \times L$) in the assumption that distribution of concentrations beyond the grain is a mirror symmetric with respect to boundaries. A homogeneous distribution with 100 small Gauss random fluctuations was taken as an initial state for simulations. The disturbance introduced by GB in the thermodynamic parameters of the alloy has a long-range nature [7] with a typical length scale ξ :

$$\Psi = \frac{\Psi_0 - \delta\Psi}{1 + x^2/\xi^2}, \quad \phi^\alpha = \frac{\phi_0^\alpha - \delta\phi}{1 + x^2/\xi^2} \quad (8)$$

where $\delta\Psi$, $\delta\phi$ are parameters specifying the disturbance amplitude, x is the distance from GB.

The influence of GB on spinodal decomposition kinetics is performed considered when alloy parameters belong to the region 3 (Fig. 1). The length R , characterizes the thickness of interphase boundary; time τ was measured in units $C_V(\omega_0^{A0} + \omega_0^{B0})/2R^2$. The results shown below were obtained at $L = 100R$, $v_0^A/v_0^B = 1$, $\xi = (1-10)R$.

3. Spinodal decomposition induced by grain boundaries

The undercooling made below spinodal curve (region 3, Fig. 1) results in alloy phase instability. In this case alloy decomposition can be provoked even by a negligible deviation in chemical potential of components near GB. Figs. 2 and 3 show typical patterns of the wave stage of SDSD (for square region—various grey shades correspond to different concentrations of A component) with disturbance of thermodynamic parameters (8) near the boundaries. As is seen, our results demonstrate more rich

decomposition kinetics than the conventional SDSD models [3–5].

Fig. 2a–c illustrate the development of SDSD when the B component segregates on GB. The structure evolution during conventional spinodal decomposition without GB is also given for comparison in Fig. 2d. The main parameter responsible for segregations at grain boundaries is $\phi^\alpha(x)$. The occurrence of segregations determines further transformation kinetics and as a result the “stripe-like” or the ordered “drop-wise” structure depending on the composition (diluted or concentrated solid solution) are realized. In Fig. 2b such process looks like an interference of plane concentration waves propagating from each boundary. This effect disappears when concentration C^{A0} increases (Fig. 2a) and plane waves become the independent modes controlling the decomposition kinetics.

The region covered by SDSD depends on the relation between concentration wave propagation velocity and decomposition rate inside grains. Hence, at small grain size the GB completely determines the morphology of precipitations (Fig. 2a–b) while for coarse grains size the ordered structure of SDSD in the boundary region coexist with “normal” SD in grain core (Fig. 2c). The deviation of energy Ψ near GB region also can lead to segregations at GB if a mean value of component concentrations C^{A0} , C^{B0} is not too close to 0.5, otherwise, according to Eq. (7), the term proportional to $\nabla\Psi$ goes to zero. Besides, the deviation of Ψ_0 from mean value leads to a local change of conditions of the solid solution stability. As seen from Fig. 3a and b fluctuations introduced in the initial concentrations distribution develop faster in the central part of a sample (Fig. 3a) or near GB (Fig. 3b) depending on the sign of additional term to mixing energy $\delta\Psi$

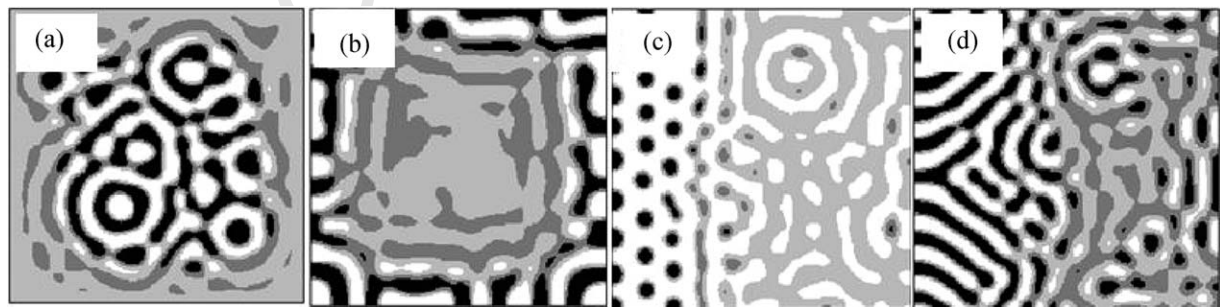


Fig. 3. Wave decomposition stage stimulated by GB; intermediate stages of decomposition with change of mixing energy near GB (a and b) and an increase (doubling) of atomic mobility of components near boundary $x = 0$ (c and d). $\Psi_0 = 8$; $\phi = 0$; $\delta\phi = 0$; $\tau = 2.5$; $\delta\Psi/\Psi_0 = 0.5$ (a), -0.5 (b), 0 (c and d); $\xi = 5R$ (a and b), $2R$ (c and d); $C^{A0} = 0.5$ (a, b and d), 0.3 (c).

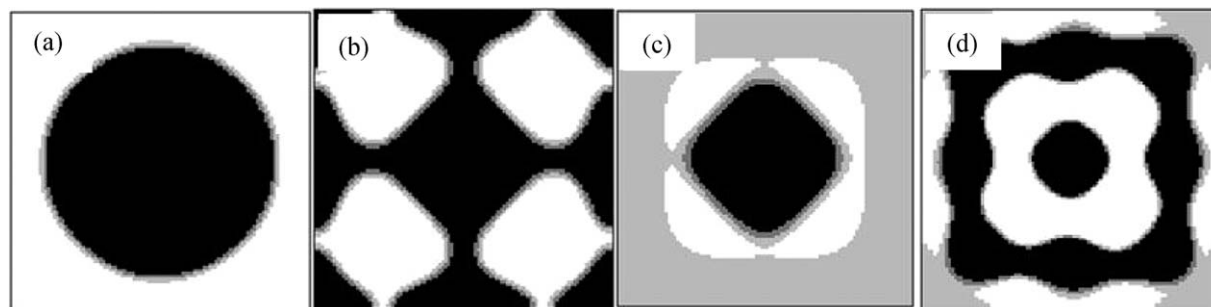


Fig. 4. Downsizing (b and d) and partial phase dissolution and component mixing (c) when GB's are introduced in a two-phase system. (a) Initial state; (b–d) $\tau = 2 \times 10^3$, $\xi = 10R$; (b) $\Psi_0 = 5$, $\phi_0 = 3$, $\delta\phi = 0.25\phi_0$; (c) $\Psi_0 = 5$, $\phi = 0$, $\delta\psi = 0.5\Psi_0$; (d) $\Psi_0 = 8$, $\phi = 0$, $\delta\psi = 0.4\Psi_0$.

near GB. The size of heterogeneous region near GB is determined by value of ξ , which is the dimensional parameter of Ψ perturbation near GB.

In Fig. 3c and d the typical patterns of wave stages of SDSD are presented for the following conditions: $\nabla\Psi = 0$, $\nabla\phi^\alpha = 0$ and frequencies ω^α near GB (located at $x = 0$) is much higher than in the grain volume. As a result, the wave stage of the spinodal decomposition first is achieved in a narrow region near GB and periodical concentrations distribution is formed along GB. This structure determines further transformation behavior and as a result, stripe-like (saturated solution) or ordered drop-like (diluted) structure is formed in the boundary adjacent region. It should be noted that the layer having a specific morphology of segregations near the boundary region is much broader than the layer in which atomic mobility of components differs from the volume one.

4. Downsizing and dissolution of precipitates in the small grains

Above we discussed the decomposition kinetics of uniform (in initial state) nanocrystalline alloys after intensive deformation. In that case the appearance of new grain boundaries can provoke the spinodal decomposition. Let us consider another case when grain size is decreased in an alloy that was previously decomposed into two-phase state as a result of SD. In this case new GB can arise inside precipitates and lead to the additional stimulus for atomic redistribution.

Fig. 4 shows the evolution of precipitates after appearance of new GB, stimulating segregations of A component at GB. It is assumed that the position of new GB coincides with boundaries of simulation box while the precipitate of A component in the initial state is in the center (Fig. 4a). As is seen, very dispersed structure can form during intermediate stages of the components redistribution (Fig. 4b). If mixing energy Ψ at GB region is lower than in grain volume and $\nabla\phi^\alpha = 0$, the initial distribution of components evolves with time towards a heterogeneous structure (Fig. 4c) in which the near-boundary region is enriched by A component ($C^A \approx 0.5$).

The most striking result is that in a certain interval of parameters the perturbation of mixing energy $\delta\psi$ introduced by GB can lead to the repetitive composition heterogeneities (Fig. 4d) similar to concentration waves accompanying SDSD. Segrega-

tion of one component (minority) provides the conditions of the beginning of SD, however, the heterogeneities near GB are to be relatively stable and with its movement from a boundary inward the grain volume, new segregations can be form near GB.

5. Conclusion

To summarize, the GB have considerable effect on the morphology of a segregated phase when state of an alloy is close to instability with respect to spinodal decomposition. In nanograin materials the development of the SDSD can be completely responsible for formation of an alloy microstructure. The variation of mixing energy can lead to a local displacement of phase equilibrium boundaries and stimulate or retard decomposition process in a near-boundary layer whose width is determined by chemical potential perturbation near GB. The increase of diffusion mobility even in a narrow layer near GB qualitatively changes the decomposition pattern in a broad region adjacent to GB. It was also shown that the formation of new GB in a two-phase state (via severe plastic deformation) can break the alloy thermodynamic equilibrium and result in decreasing of segregations size and their dissolution.

Acknowledgments

This work was supported by the Program of Basic Research of the Presidium of the Russian Academy of Sciences "The fundamental problems of physics-chemistry of nanomaterials" and Integration Program between SB and UB of RAS.

References

- [1] J.W. Christian, Transformations in Metals and Alloys, Part I, 2nd ed., Pergamon Press, 1975.
- [2] K. Binder, in: R.W. Cahn, P. Haasen, J. Kramer (Eds.), Phase Transformations of Materials, VCH, Weinheim, 1991.
- [3] S. Puri, H.L. Frisch, J. Phys.: Cond. Mater. 9 (1997) 2109.
- [4] H. Ramanarayan, T. Abinandanan, Acta Mater. 51 (2003) 4761; H. Ramanarayan, T. Abinandanan, Acta Mater. 52 (2004) 921.
- [5] B. Aichmayer, P. Fratzl, S. Puri, G. Saller, Phys. Rev. Lett. 91 (2003) 015701.
- [6] A.Y. Yermakov, Mater. Sci. Forum 179–181 (1995) 455.
- [7] Y.N. Gornostyrev, I.K. Razumov, A.Y. Yermakov, J. Mater. Sci. 39 (2004) 5003.
- [8] A.Y. Yermakov, V.L. Gapontsev, V.V. Kondratyev, Y.N. Gornostyrev, Phys. Met. Metallogr. 88 (1999) 211.

- 259 [9] R.Z. Valiev, I.V. Aleksandrov, Nanostructurnie materiali, poluchennie
260 intensivnoj plasticheskoj deformaciej, Logos, Moscow, 2000 (in Russian). 262
261 [10] K.P. Guroff, Processi vzaimnoj diffuzii v splavah, Nauka, Moscow, 1973, 263
p. 360. 264
- [11] J.-F. Gouyet, M. Plapp, W. Dieterich, P. Maass, Adv. Phys. 52 (2003) 523.
[12] V.G. Vaks, Phys. Rep. 391 (2004) 157.
[13] Cahn S J.W., J.E. Hillard, J. Chem. Phys. 31 (1959) 688.

UNCORRECTED PROOF